B BRAUN
SHARING EXPERTISE

SPINE SURGERY

AESCULAP® CeSPACE® 3D

CERVICAL INTERBODY FUSION SYSTEM

SURGICAL MANUAL

AESCULAP® CERVICAL SPINE

PROTECTING AND PRESERVING SPINAL STABILITY

Modern lifestyle has resulted in increasing physical inactivity among people all over the world. Of the many medical problems associated with this, spinal disorders are among the most critical. This is even more significant as the spinal column is one of the most important structures in the human body. It supports and stabilizes the upper body and is the center of our musculoskeletal system, which gives the body movement.

Our work in the field of spine surgery is dedicated to protecting the spinal column and preserving its stability. We support spine surgeons with durable, reliable products and partner services for proven procedures and good clinical outcomes (1-10).

Our philosophy of sharing expertise with healthcare professionals and patients allows us to develop innovative implant and instrument systems that help to preserve stability and stabilize the cervical and thoracolumbar spine.

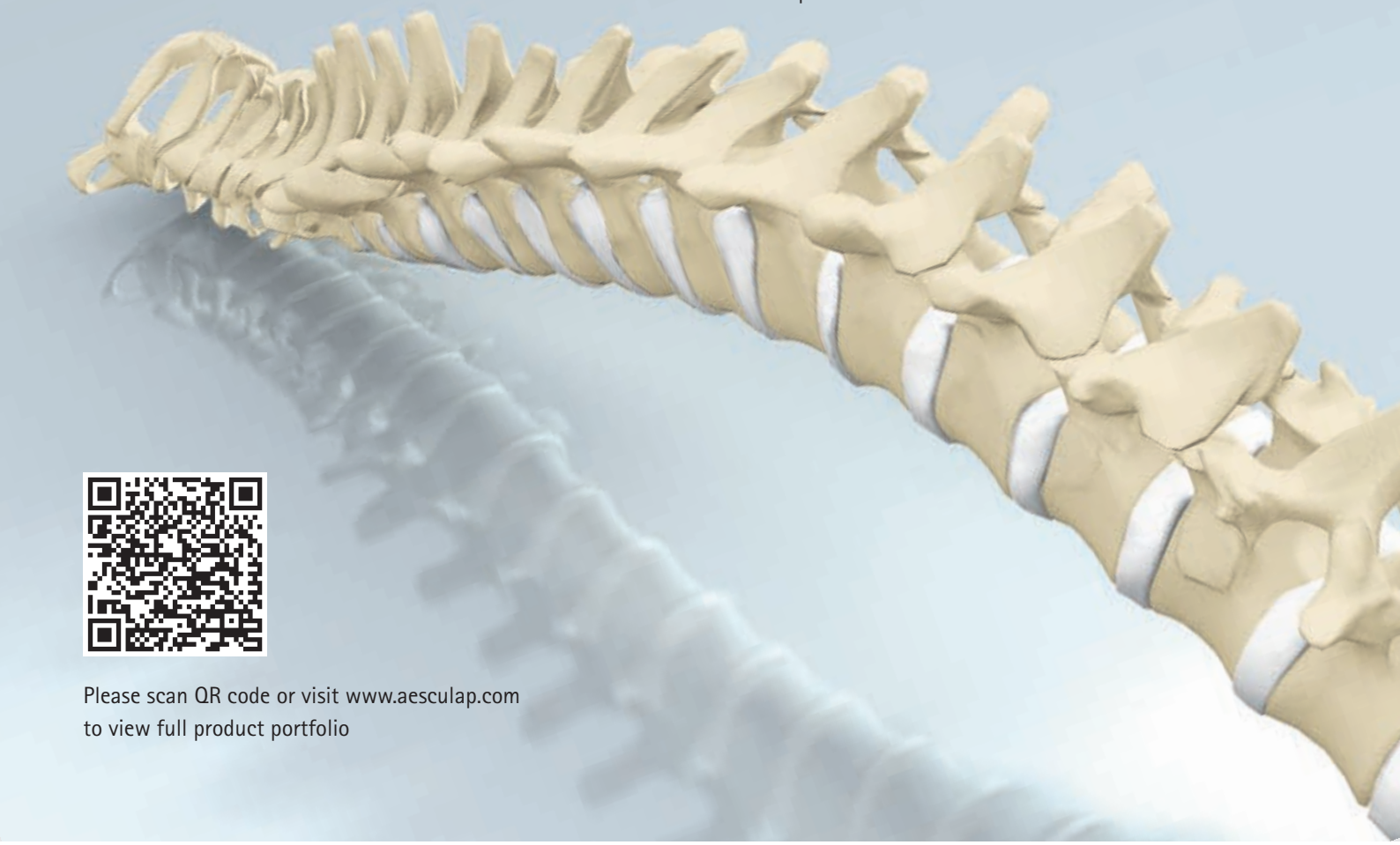

Please scan QR code or visit www.aesculap.com to view full product portfolio

AESCULAP® CeSPACE® 3D

CONTENT

IMPLANT MATERIAL

AESCULAP® 3D Cages

Fig. 1: Laser beam melting technology

THE TECHNOLOGY OF LASER SINTERING – A WELL-ESTABLISHED ADDITIVE LAYER BY LAYER PROCESS

Additive manufacturing – 3D printing – means a layer by layer process to design a device using laser beam and metal powder. This innovative laser beam melting technology is of growing importance in the manufacture of implants, as it allows to create various fine and porous surface structures with the aim to support bone-ingrowth. Homogenous or heterogeneous lattice structures or combinations of various kinds of structures and surfaces are generally conceivable.

- Direct assembly of the component based on 3D-CAD data
- Design freedom

We combined our long-time experience in designing and manufacturing spinal implants with latest technology and produce in-house our AESCULAP® 3D Cages (Fig. 1).

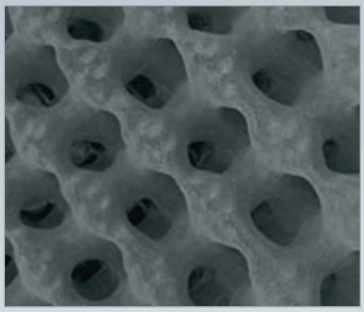

Fig. 2: Lattice structure Structan® of AESCULAP® 3D Cages

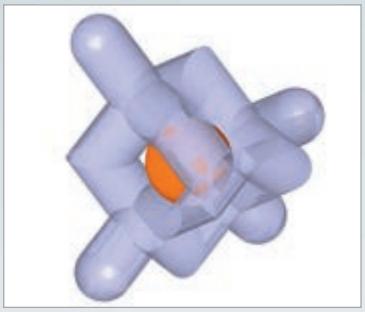

Fig. 3: Unit cell with fitted ball of 900 µm (pore size)

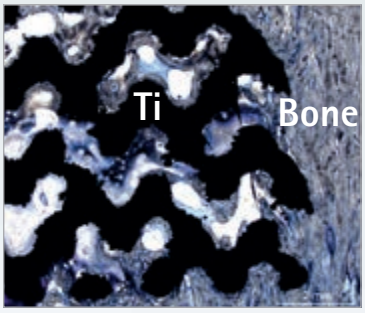

Fig. 4: Histological section of the 3D Cage lattice structure filled with newly formed bone

AESCULAP® 3D Cages are engineered from Structan® – a lattice structure with largely isotropic behavior. Ti6Al4V ELI was chosen as a proven and biocompatible material for implants (11).

MORE CONNECTION

- The lattice structure of the AESCULAP® 3D Cages shows an interconnected pore structure (Fig. 2, 3). This interconnectivity facilitates migration of bone cells into the structure, thereby providing secondary stability (12, 13).
- According to the average pore size and porosity of cancellous bone (approximately 1 mm / 50 - 90 % (14)) the 3D lattice structure Structan® features an all-over regular pore size of 900 µm as well as a mean interconnected porosity of 50 - 55 %. Pore size and porosity are in a favorable range to stimulate bone in-growth (15, 16).
- The results of a sheep study with partly loaded implants confirm bone growth on and into the 3D lattice structure without connective tissue layer six months postoperatively. This formation of bone tissue within the 3D lattice structure leads to a high secondary stability (13). The 3D lattice structure serves as a guide rail for bony integration and thus contributes significantly to the secure anchoring of the 3D Cage (Fig. 4).
- A rough laser sintered surface provides a good interaction between bone cells and implant surface compared to a milled smooth surface and therefore intends to optimize osseointegration (17).

IMPLANT MATERIAL

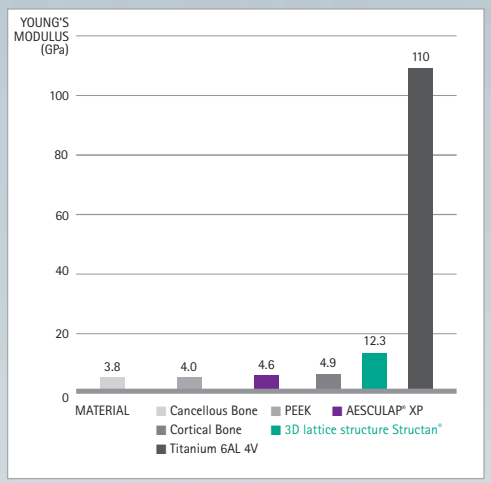

Fig. 5: Young's modulus of various materials

MORE ELASTICITY

- Ti6Al4V ELI as solid material has a Young's modulus of approximately 110 GPa as it is shown in the figure, whereas cortical bone has a Young's modulus of approximately 5 GPa (18, 19).
  The Young's modulus of Structan® is developed to be close to that of cortical bone. This may prevent subsidence into the vertebral body (20). In addition, this may result in improved bone growth (21) (Fig. 5).

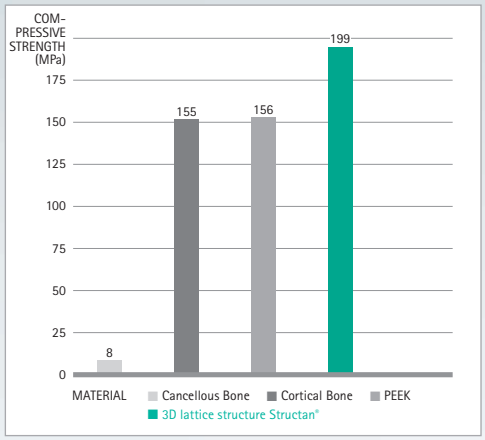

Fig. 6: Compressive strength of 3D lattice structure Structan®

MORE STRENGTH

- The 3D lattice structure Structan® combines a bone-like Young's modulus with a high compressive strength, which contributes to high safety against failure due to breakage.
  The compressive strength of the 3D lattice structure Structan® is higher than the mean strength of bone and PEEK (22, 23) (Fig. 6).

INTENDED USE

CeSPACE® 3D

- Stabilization of the cervical spine C2-T1 through anterior approach, monosegmental and multisegmental.
- A cervical plate may be required for additional stabilization.

IMPLANT DESIGN

- Solid frame without sharp edges for biomechanical stability and smooth insertion into the disc space minimizing the risk to injure surrounding soft tissue.
- Open porous structure designed to provide primary and secondary stability.
- The implant's anatomical endplate design provides a good contact area between implant and vertebral endplates whilst allowing addition of bone material to enable bone growth through the center of the implant.
- Cranial und caudal anchoring elements in form of spikes for a firm implant fit and high primary stability.
- Trapezoidal shape intended to fit anatomical conditions.
- Screw thread interface allows a firm connection to inserter.
- Good visibility in X-ray to localize implant positioning (24, 25).

AESCULAP® CeSPACE® 3D

B | SURGICAL TECHNIQUE

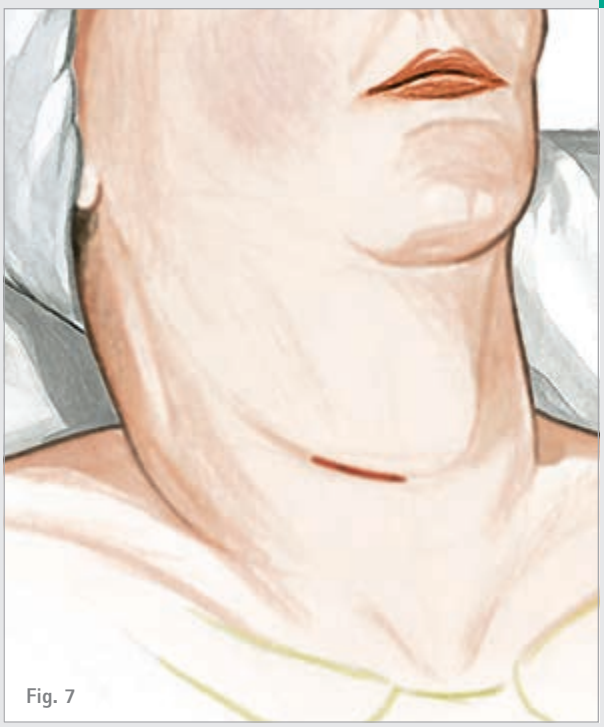

Fig. 7

Fig. 8

B.1. PATIENT POSITIONING

- The patient is placed in the supine position with the head slightly reclined and stabilized in a head holder (Fig. 7). Once the lordotic cervical spine has been supported, the thorax may be placed on a pillow to emphasize the reclination of the cervical spine. The arms are fixed alongside the body.

B.2. EXPOSURE OF THE INTERVERTEBRAL SPACE

- After the skin incision and preparation, the CCR retractor is placed. The blades are available in PEEK and titanium (Fig. 8). A counter retractor can be used. The subcutaneous tissue is separated from the platysma cranially, caudally and medially, and the platysma is also separated following the direction of its fibres. The margins of the platysma can be held apart with the retractor or with two surgical forceps.
- Now the medial edge of the sternocleidomastoid muscle is located and prepared with the index finger in the connective tissue space over the ventral surface of the cervical spine and under lateralization of the vascular nerve bundle and medialization of the trachea, esophagus and thyroid gland.
- After the Langenbeck hooks have been inserted, the ventral surface of the cervical spine, still covered by a thin prevertebral layer of connective tissue, is revealed. This layer can now be exposed by either a blunt scissor or alternatively through bipolar coagulation, in order to expand the tissue cranially and caudally using a swab. A wire is set under X-ray monitoring to mark the intervertebral disc space.

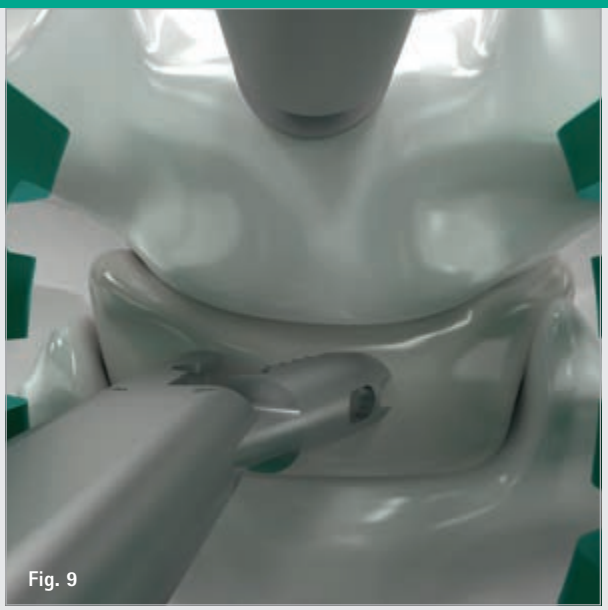

Fig. 9

B.3. DISTRACTION / DISCECTOMY / PREPARATION OF THE ENDPLATES

- The distraction screws are placed in position and the CASPAR® distractor is applied following the CASPAR® technique (Fig. 8). Complete discectomy is performed using various rongeurs, rectangular curettes and bone curettes (Fig. 9). While using a high speed drill to remove the posterior rim and / or dorsal osteophytes, care must be taken to avoid damaging the vertebral body endplates.

PLEASE NOTE

› Make certain that the endplates of the neighboring vertebral bodies are not weakened, in order to minimize the risk of migration.

› Make certain that the implant bed is properly prepared to avoid damage to the implant when it is driven in.

Fig. 10

B.4. ASSEMBLING OF THE TRIAL IMPLANTS

- The depth stop is snapped onto the shaft of the trial implant (Fig. 10).
- Markings on the depth stop indicate the correct assembling.

PLEASE NOTE
Use CeSPACE® 3D trial implant with depth stop.

Fig. 11/12

B.5. IMPLANT SELECTION

- Use trial implants to establish the correct implant size.
- When inserting the trial implant observe the markings to correctly align the trial implant. Markings on the handle as well as on the trial itself indicate the cranial side of the trial (Fig. 11/12).

DETERMINATION OF IMPLANT SIZE
The CeSPACE® 3D trials have the anatomical shape of the CeSPACE® 3D implants.

PLEASE NOTE
The trials are essential to ensure the correct implant size to be used.

Fig. 13

B.6. IMPLANT REMOVAL FROM PACKAGING

- Open folder blister to remove the CeSPACE® 3D implant.
- The packaging concept allows implant removal with the connected inserter.

B.7. ASSEMBLING OF THE INSERTION INSTRUMENT

- The depth stop is snapped onto the shaft of the insertion instrument. It prevents the implant from being inserted too deeply into the intervertebral disc compartment (Fig. 13).

PLEASE NOTE
Use CeSPACE® 3D Insertion instrument with depth stop.

Fig. 14

B.8. FILLING OF CAGE

- Use the packing block and the punch for optional filling of the implant with bone or bone substitute (Fig. 14).
- The CeSPACE® 3D implant is connected with the inserter.

PLEASE NOTE
Do not use force during filling to avoid implant damaging.

Fig. 15

Fig. 16

B.9. CeSPACE® 3D INSERTION

- The CeSPACE® 3D implant is held securely and firmly onto the CeSPACE® inserter by means of a screw joint (Fig. 15).
- Once CeSPACE® 3D is attached to the inserter, it can be introduced into the intervertebral space using image converter monitoring (Fig. 16).
- When inserting the implant into the intervertebral space, observe the markings to correctly align the implant.

PLEASE NOTE
Implant marking points in the cranial direction.

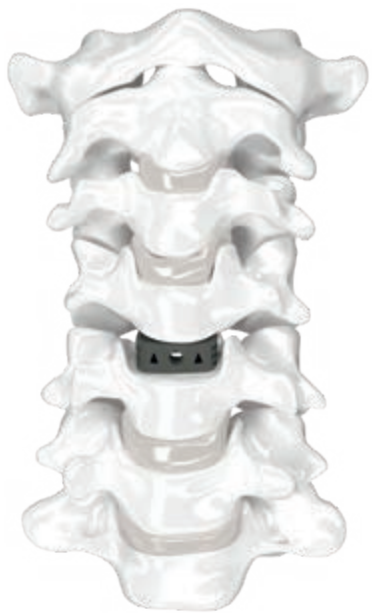

Fig. 17

B.10. FINAL POSITIONING

- The implant should be inserted centrally in AP and with a distance of approximately 1 - 2 mm to both the anterior and posterior rim (Fig. 17).
- For additional stabilization, a cervical plate may be necessary.

AESCULAP® CeSPACE® 3D

C | IMPLANT & INSTRUMENT OVERVIEW

CeSPACE® 3D IMPLANTS, 5°

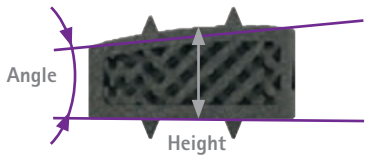

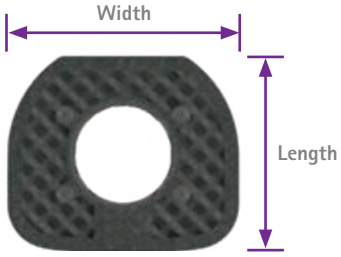

Article No.	Size (Height x Width x Length)	Quantity
SN634T	4 x 14 x 11.5 mm	2
SN635T	5 x 14 x 11.5 mm	2
SN636T	6 x 14 x 11.5 mm	2
SN637T	7 x 14 x 11.5 mm	2
SN638T	8 x 14 x 11.5 mm	2
SN644T	4 x 16 x 13.5 mm	2
SN645T	5 x 16 x 13.5 mm	2
SN646T	6 x 16 x 13.5 mm	2
SN647T	7 x 16 x 13.5 mm	2
SN648T	8 x 16 x 13.5 mm	2
SN654T	4 x 18 x 15 mm	2
SN655T	5 x 18 x 15 mm	2
SN656T	6 x 18 x 15 mm	2
SN657T	7 x 18 x 15 mm	2
SN658T	8 x 18 x 15 mm	2

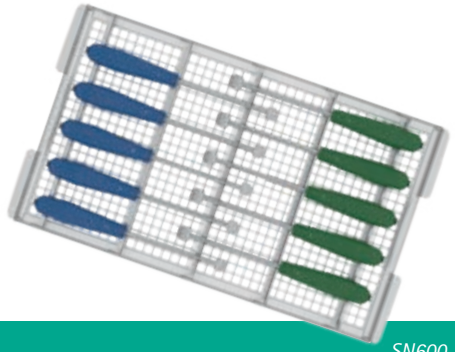

SN600 – CeSPACE® 3D Instrumentation

SN600
CeSPACE® 3D Implantation

INSTRUMENTS	Article No.	Description	Quantity
	SN601R	CeSPACE® 3D Tray F/Instrumentation	1
	TF363	Graphic template F/SN601R (SN600)	1
	TF353	Packing Stencil F/SN601R (SN600)	1
	JA455R	Lid for OrthoTray DIN W/O Handle	1
	**SN664R**	CeSPACE® 3D trial implant 5°, 4 x 14 x 11.5 mm	1
	SN665R	CeSPACE® 3D trial implant 5°, 5 x 14 x 11.5 mm	1
	SN666R	CeSPACE® 3D trial implant 5°, 6 x 14 x 11.5 mm	1
	SN667R	CeSPACE® 3D trial implant 5°, 7 x 14 x 11.5 mm	1
	SN668R	CeSPACE® 3D trial implant 5°, 8 x 14 x 11.5 mm	1
	**SN674R**	CeSPACE® 3D trial implant 5°, 4 x 16 x 13.5 mm	1
	SN675R	CeSPACE® 3D trial implant 5°, 5 x 16 x 13.5 mm	1
	SN676R	CeSPACE® 3D trial implant 5°, 6 x 16 x 13.5 mm	1
	SN677R	CeSPACE® 3D trial implant 5°, 7 x 16 x 13.5 mm	1
	SN678R	CeSPACE® 3D trial implant 5°, 8 x 16 x 13.5 mm	1

AESCULAP® CeSPACE® 3D

C | IMPLANT & INSTRUMENT OVERVIEW

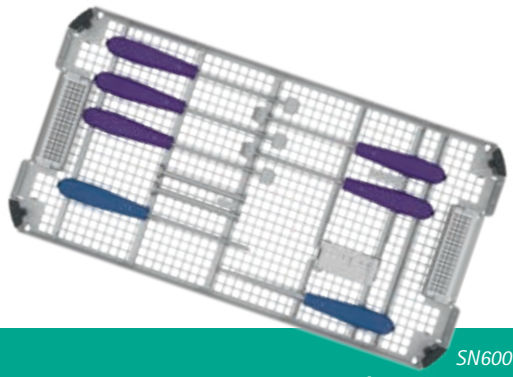

SN600
CeSPACE® 3D Implantation

SN600 CeSPACE® 3D Instrumentation

INSTRUMENTS	Article No.	Description	Quantity
	**SN684R**	CeSPACE® 3D trial implant 5°, 4 x 18 x 15 mm	1
	SN685R	CeSPACE® 3D trial implant 5°, 5 x 18 x 15 mm	1
	SN686R	CeSPACE® 3D trial implant 5°, 6 x 18 x 15 mm	1
	SN687R	CeSPACE® 3D trial implant 5°, 7 x 18 x 15 mm	1
	SN688R	CeSPACE® 3D trial implant 5°, 8 x 18 x 15 mm	1
	**SN663R**	CeSPACE® 3D depth stop	2
	**SN604R**	CeSPACE® 3D packing block	1
	**FF913R**	CASPAR® Graft positioning tamp – 3 mm diameter	1
	**SN605R**	CeSPACE® 3D insertion instrument	1

Recommended container: JK441
Recommended container lid: JK489
Recommended identification label: JG790B

REFERENCE

(1) Suchomel P, Jurák L, Antinheimo J, Pohjola J, Stulik J, Meisel HJ, et al. Does sagittal position of the CTDR-related centre of rotation influence functional outcome? Prospective 2-year follow-up analysis. Eur Spine J. 2014 May;23(5):1124-34.

(2) Meisel HJ, Jurák L, Antinheimo J, Arregui R, Bruchmann B, Čabraja M, et al. Four-year results of a prospective single-arm study on 200 semi-constrained total cervical disc prostheses: clinical and radiographic outcome. J Neurosurg Spine. 2016 Jun;3:1-10.

(3) Boselie TFM, van Santbrink H, de Bie RA, van Mameren H. Pilot Study of Sequence of Segmental Contributions in the Lower Cervical Spine During Active Extension and Flexion: Healthy Controls Versus Cervical Degenerative Disc Disease Patients. Spine (Phila Pa 1976). 2017 Jun 1;42(11):E642-E647.

(4) Epstein NE. Anterior cervical dynamic ABC plating with single level corpectomy and fusion in forty-two patients. Spinal Cord. 2003 Mar;41(3):153-8. PubMed PMID:12612617.

(5) Stulik J, Pitzen TR, Chrobok J, Ruffing S, Drumm J, Sova L, et al. Fusion and failure following anterior cervical plating with dynamic or rigid plates: 6-months results of a multicentric, prospective, randomized, controlled study. Euro Spine J. 2007;16:1689-94.

(6) Krayenbühl N, Schneider C, Landolt H, Fandino J. Use of an empty, Plasmapore-covered titanium cage for interbody fusion after anterior cervical microdiscectomy. J Clin Neurosci. 2008; 15(1):11-7.

(7) Takeuchi M, Yasuda M, Niwa A, Wakao N, Nakura T, Osuka K, et al. Plasmapore-coated titanium cervical cages induce more rapid and complete bone fusion after anterior cervical discectomy and fusion as compared to noncoated titanium cage. World Neurosurg. 2014;82(3-4):519-22.

(8) Stulik J, Vyskocil T, Sebesta P, Kryl J. Atlantoaxial fixation using the polyaxial screw-rod system. Eur Spine J. 2007 Apr; 16(4):479-84. PubMed PMID: 17051397; PubMed Central PMCID: PMC2229812.

(9) Tippets RH, Apfelbaum RI. Anterior cervical fusion with the Caspar instrumentation system. Neurosurgery. 1988 Jun; 22(6 Pt 1):1008-13. PubMed PMID: 3419561.

(10) Stulik J, Nesnidal P, Kryl J, Vyskocil T, Barna M. Kyphotic deformities of the cervical spine. 28th Annual Meeting of the AANS/CNS Section on Disorders of the cervical Spine and peripheral Nerves. March 2012 Orlando, Florida.

(11) Ngoc Bich VU, et al. In vitro and in vivo biocompatibility of Ti-6Al-4V titanium alloy and UHMWPE polymer for total hip replacement. Biomedical Research and Therapy. 2016;3(3):567-77.

(12) Van der Stok J, Van der Jagt O, Yavari S, De Haas M, Waarsing J, Jahr H, et al. Selective laser melting-produced porous titanium scaffolds regenerate bone in critical size cortical bone defects. Journal of Orthopaedic Research 2013;31(5):792–9.

(13) In vivo study of porous metallic lattice structures, Ulm, 2019. The biocompatibility, osseointegration and biomechanical properties of porous Ti6Al4V implants manufactured by SLM were tested under mechanical loading conditions in an ovine model study sponsored by Aesculap AG. The samples were evaluated histologically and biomechanically after implantation. Porous Ti6Al4V implants exhibited very good biocompatibility, bone-implant interface strength and osseointegration. Six months after implantation, bone ingrowth on and into the porous Ti6Al4V implants was reported. Inflammatory reactions that may influence bone formation were not observed.

REFERENCE

(14) Karageorgiou V, Kaplan D. Porosity of 3D biomaterial scaffolds and osteogenesis. Biomaterials. 2005;26(27):5474-91.

(15) Taniguchi N, et al. Effect of pore size on bone ingrowth into porous titanium implants fabricated by additive manufacturing: an in vivo experiment. Materials Science and Engineering: C. 2016;59:690-701.

(16) van Bael S, et al. The effect of pore geometry on the in vitro biological behavior of human periosteum-derived cells seeded on selective laser-melted Ti6Al4V bone scaffolds. Acta biomaterialia. 2012;8(7):2824-34.

(17) Elias CN, et al. Mechanical and clinical properties of titanium and titanium-based alloys (Ti G2, Ti G4 cold worked nanostructured and Ti G5) for biomedical applications. Journal of Materials Research and Technology. 2019;8(1):1060-9.

(18) Kuhn JL, Goldstein SA, Choi K, London M, Feldkamp LA, Matthews LS. Comparison of the trabecular and cortical tissue moduli from human iliac crests. J Orthop Res. 1989;7(6):876-84.

(19) Ratner BD, Hoffmann AS, Schoen FJ, Lemons JE. An Introduction to Materials in Medicine. Academic Press. 1996

(20) Chen Y, Wang X, Lu X, Yang L, Yang H, Yuan W, et al. Comparison of titanium and polyetheretherketone (PEEK) cages in the surgical treatment of multilevel cervical spondylotic myelopathy: a prospective, randomized, control study with over 7-year follow-up. Eur Spine J. 2013;22(7):1539–46.

(21) Brizuela A, et al. Influence of the elastic modulus on the Osseointegration of Dental Implants. Materials. 2019;12(6):980.

(22) Azami M, Moztarzadeh F, Tahriri M. Preparation, characterization and mechanical properties of controlled porous gelatin/hydroxyapatite nanocomposite through layer solvent casting combined with freeze-drying and lamination techniques. Journal of Porous Materials. 2010;17(3):313-20.

(23) Rae PJ, Brown EN, Orler EB. The mechanical properties of poly (ether-ether-ketone) (PEEK) with emphasis on the large compressive strain response. Polymer. 2007;48(2):598-615.

(24) Usability-Test, Usability Validation of AESCULAP® CeSPACE® 3D Cages, Tübingen, 2019.
The usability of the AESCULAP® 3D Cage System CeSPACE® 3D was tested in April 2019, in a cadaver workshop with six independent test persons as intended users (surgeons specialized in spinal surgery or comparable fields). Parameters such as implant visibility under x-ray control, mechanical stability of the implant/instrument interface and implant surface evaluation in terms of tissue injury risk were tested among others. Acceptance criteria were fulfilled for all the above-mentioned parameters. All test users confirmed the absence of critical features that must be improved prior to clinical use. During the test, the x-ray visibility of the cages was particularly positively assessed.

(25) Rehnitz, Christoph, PD Dr. med. Radiological image evaluation of AESCULAP® interbody fusion devices, Heidelberg, 2019.
CT and X-ray visualization of different AESCULAP® interbody fusion cages (full titanium, porous Ti6Al4V and PLASMAPORE$^{XP®}$ cages) was tested in a cadaver setup. A radiologist evaluated the implant visibility and the presence of artefacts that may limit the visualization of adjacent structures. Visualization and assessment of implant position was achieved in X-ray and CT for all tested cages. Minor artefacts were visible in CT reconstructions in the surrounding of porous Ti6Al4V and full titanium implants. Porous Ti6Al4V implants showed slightly fewer artefacts in CT in comparison to full titanium implants. The minor artefacts observed did not limit the assessment of the surrounding anatomical structures.

AESCULAP® – a B. Braun brand

Aesculap AG | Am Aesculap-Platz | 78532 Tuttlingen | Germany
Phone +49 7461 95-0 | Fax +49 7461 95-2600 | www.aesculap.com

003002 0520/PDF/1